INSTITUT NATIONAL DE RECHERCHE EN INFORMATIQUE ET EN AUTOMATIQUE

Using models of dynamics for large displacement estimation on noisy acquisitions

Dominique Béréziat — Isabelle Herlin

N° 7408

Octobre 2010

Thème NUM

Rapport de recherche

ISSN 0249-6399 ISRN INRIA/RR--7408--FR+ENG

INSTITUT NATIONAL
DE RECHERCHE
EN INFORMATIQUE
ET EN AUTOMATIQUE

INRIA

centre de recherche
PARIS - ROCQUENCOURT

Using models of dynamics for large displacement estimation on noisy acquisitions

Dominique Béréziat* , Isabelle Herlin†

Thème NUM — Systèmes numériques
Équipes-Projets CLIME

Rapport de recherche n° 7408 — Octobre 2010 — 15 pages

Abstract:

The paper discusses the issue of motion estimation on noisy images displaying large displacements, due to high velocity values. "Noisy" means that the data contain either missing acquisitions on isolated points, regions, frames or noisy measures. Assuming the dynamics is partially accessible from heuristics and modeled, the objective is to include this knowledge in the computation of the solution even if large displacements occur from one frame to the next one and if the data are noisy. This is performed by Data Assimilation techniques which simultaneously solve an evolution equation and an observation equation. The evolution equation includes the partial knowledge on the dynamics. The observation equation describes the transport of image brightness and is written in a non-linear form in order to better characterize large displacements. The assimilation method is a weak 4D-Var algorithm, in which each component of the Data Assimilation system is associated to an error. We prove that the observation covariance matrix can be used to discard the noisy data during the computation of the solution letting the evolution equation estimate motion from adjacent frames on these pixels. The method is quantified on synthetic data and illustrated on oceanographic satellite images.

Key-words: variational data assimilation, optical flow, large displacements, noisy or missing data, SST images

* Université Pierre et Marie Curie, LIP6, 4 place Jussieu, 75005 Paris, France
† INRIA, CEREA, Joint Laboratory ENPC-EDF R&D, Université Paris-Est

Centre de recherche INRIA Paris – Rocquencourt
Domaine de Voluceau, Rocquencourt, BP 105, 78153 Le Chesnay Cedex
Téléphone : +33 1 39 63 55 11 — Télécopie : +33 1 39 63 53 30

Utilisation de modèles de la dynamique pour l'estimation de larges déplacements sur des acquisitions bruitées

Résumé : Cet article traite du problème de l'estimation du mouvement sur des données bruitées montrant de grands déplacements engendrés par des vitesses élevées. Par données "bruitées" nous entendons des données qui contiennent à la fois des informations manquantes en des points isolés, des régions ou des plans image entiers et du bruit de mesure. En supposant que la dynamique de la séquence d'image peut être décrite par des heuristiques, le but est d'inclure cette connaissance dans le calcul de la solution et cela malgré la présence de vitesses élevées. Ceci est réalisé par assimilation de données en résolvant simultanément une équation d'évolution et une équation d'observation. L'équation d'évolution décrit imparfaitement la dynamique. L'équation d'observation décrit le transport de la luminosité par la vitesse et elle est écrite sous sa forme non linéaire afin de prendre en compte les grands déplacements. La méthode d'assimilation de données utilisée ici est le "4DVar" dans sa formulation faible et pour laquelle chaque composante du système à résoudre est associée à une erreur. Nous montrons que la matrice de covariance associée au modèle d'observation peut être utilisée pour éliminer du calcul de la solution les pixels qui contiennent une information bruitée. Pour ces pixels, l'équation d'évolution permet alors de calculer une solution admissible. La méthode proposée est évaluée sur des données synthétiques et appliquée sur des données océanographiques contenant de véritables données manquantes.

Mots-clés : assimilation variationnelle de données, flot optique, large déplacements, données bruitées ou manquantes, images SST

1 Introduction

Motion estimation is one major task of Image Processing. It is applied for instance on satellite data to study the cloud structures dynamics or to estimate the ocean surface circulation. In the medical domain, motion detection is used for analyzing the dynamics of organs: abnormalities of the cardiac cycle are detected with ultrasound imaging and the brain neural activity is controlled with magneto and electroencephalography (MEG/EEG) or magnetic resonance imaging (MRI). In video surveillance, motion information permits to assess people behavior.

Motion vectors fields are often inferred from the Optical Flow Constraint Horn and Schunk (1981) but this equation is only valid for small displacements as it results from the linearization of a non linear equation. However, large displacements frequently occur if the time period of the acquisition process is too large compared to the observed dynamics. There are two main approaches to deal with this issue. The first one solves the Optical Flow Constraint equation with an incremental algorithm Odobez and Bouthemy (1998); Proesmans et al. (1994), each iteration remaining a linear problem. The second one directly solves the non linear equation of image brightness transport. Such method is named warping method Brox et al. (2004).

An additional difficulty concerns the quality of images: as widely known, the image data are commonly noisy. This degradation has various origins: a failing acquisition process, occluding structures (clouds over the sea, people behind objects, ...), or a poor quality of the signal (ultrasound imaging for instance). The corresponding values should be ignored or given a low weight during the estimation process and the final result.

Estimating a motion field from two consecutive images with the optical flow constraint is an ill-posed problem and additional information must be provided to obtain a unique solution. Usually the uniqueness is obtained by constraining the space of the solutions. This method, named Tikhonov regularization, is widely used in the literature Tikhonov (1963). However, this is too restrictive and not always justified according to the experimental context.

Sometimes the underlying dynamics is partially known. This is the case if the physical processes, visualized on images, are accurately modeled by the specialists. In meteorology and oceanography, equations, approximately describing apparent motion on the image data, can be derived from the fluid flow dynamics. In the medical domain, efforts are engaged to describe the electro-mechanic cardiac cycle and the brain electric activity, and first dynamic models are now available. The problem is then to include this knowledge in the computation of the solution: this is achieved using Data Assimilation methods. Knowing the approximate dynamics provides two major advantages as it had been discussed in Bérériat and Herlin (2010): first, a unique solution can be obtained without any Tikhonov regularisation and, second, a solution is obtained even if the observation are noisy. Using Data Assimilation to determine motion from image sequences is an emerging domain. In Papadakis et al. (2007a), the optical flow constraint is used as observation equation to compute velocity and two alternative evolution equations are considered: a Navier-Stokes equation ruling the fluid velocity and a transport of velocity by itself for addressing rigid motions. In Papadakis et al. (2007b), the velocity field of several atmospheric layers is computed from pressure images and shallow-water equations are used as evo-

lution equation for velocity and pressure. In Huot et al. (2008), the surface velocity field is estimated from SST images with a shallow-water model and an advection/diffusion equation for the temperature.

In this paper, the issue of motion estimation is investigated in the following context: the displacements may be large and approximately ruled by the transport of brightness; observations may be noisy but the localization of noisy pixels is known by the user from metadata. Without any information on the image dynamics, the transport of velocity by itself is considered. Such assumption means that the motion vector is constant over time along the pixel trajectory. As this model is rough, derivation from it is accepted in the estimation process. In Section 2, the issue of motion estimation is introduced, and equations ruling the evolution of brightness and the dynamics are discussed. In Section 3, the variational data assimilation framework is briefly described for a complete understanding of our method. Section 4 gives a discussion about the covariance matrix associated to the error involved in the observation equation. We explain how to use it to discard noisy data from the solution and to add spatio-temporal regularity constraints on the solution. In Section 5, results are quantified on synthetic images and displayed on SST data acquired over the Black Sea. Concluding remarks and perspectives are given in Section 6.

2 Defining the evolution over the image sequence

Optical flow measures the displacement of patterns on a sequence of images. This is one signature of the physical processes occurring in the scene during the acquisition. Equations ruling it therefore depend on the studied context. A first example concerns the estimation of fluid particles velocity from a mass conservation equation:

$$\frac{\partial I}{\partial t} + \nabla^T (I\mathbf{V}) = 0 \tag{1}$$

with I denoting the image value, ∇ the spatial gradient, ∇^T its transpose and $\mathbf{V}$ the velocity. This equation is suitable if, for instance, I is an image of pressure and $\mathbf{V}$ the blood speed Wildes and Amabile (1997) or I is an image of temperature (satellite infrared image) and $\mathbf{V}$ the clouds displacement Béréziat et al. (2000); Isambert et al. (2008). A second example, commonly used for video sequences, assumes that moving objects display a Lambertian surface and the optical flow is modeled as the transport of image brightness by the velocity vector:

$$I(\mathbf{x} + \mathbf{V}(\mathbf{x};t)\triangle t; t + \triangle t) = I(\mathbf{x};t)$$

$\mathbf{x}$ and t are space-time coordinates, $\triangle t$ is the time step between two frames and can be set to 1 without any loss of generality:

$$I(\mathbf{x} + \mathbf{V}(\mathbf{x};t); t+1) = I(\mathbf{x};t) \tag{2}$$

Being non linear, Equation (2) is commonly approximated by a first-order Taylor expansion:

$$\frac{\partial I}{\partial t} + \nabla I^T \mathbf{V} = 0 \tag{3}$$

Equations (1), (2) and (3) are named *observation equations* as they link the observations and the quantity to be computed, named the state vector, which

is the velocity field $\mathbf{V}$.
As we are interested in tracking structures visualized on the ocean surface, the displacements may be large if the time period between two frames is high compared to the dynamics time scale. Equation (3) is then no more valid and Equation (2) is considered. This observation equation is not invertible and provides an infinity of solutions. A first possibility to overcome this difficulty is to look for the velocity $\mathbf{V}$ as the minimum of an objective function and to include a constraint on the velocity spatial variation. This is named the Tikhonov regularization Tikhonov (1963):

$$\int \left((I(\mathbf{x}+\mathbf{V};t+1) - I(\mathbf{x};t))^2 + \alpha^2 \|\nabla \mathbf{V}\|^2 \right) d\mathbf{x} \tag{4}$$

The associated Euler-Lagrange equation is established and leads to a non linear system. A semi-implicit scheme Brox et al. (2004) can then be used with the drawback of requiring the inversion of a large matrix. A second possibility is to consider an incremental method such as in Proesmans et al. (1994). In this case, we consider the value $I(\mathbf{x}+\tilde{\mathbf{V}};t+1)$ with $\tilde{\mathbf{V}}$ being the current estimate of the velocity $\mathbf{V}$, and subtract it in Equation (2). We obtain after a first-order Taylor expansion:

$$\nabla I^T(\mathbf{x};t)(\mathbf{V}-\tilde{\mathbf{V}}) + I(\mathbf{x}+\tilde{\mathbf{V}};t+1) - I(\mathbf{x};t) = 0 \tag{5}$$

This equation is also ill-posed and requires a Tikhonov regularization. The new objective function is:

$$\int \left(\nabla I^T(\mathbf{V}-\tilde{\mathbf{V}}) + I(\mathbf{x}+\tilde{\mathbf{V}};t+1) - I)^2 + \alpha^2 \|\nabla \mathbf{V}\|^2 \right) d\mathbf{x} \tag{6}$$

Equation (5) being linear, the Euler-Lagrange equation associated to (6) is linear and can be solved efficiently with a Gauss-Seidel method Horn and Schunk (1981). It provides a solution for $\mathbf{V}$ from the estimate $\tilde{\mathbf{V}}$. Due to the Taylor expansion, the equation provides an approximate solution of the transport equation (2). The process is then iterated until convergence using the solution from an iteration as the initial estimate for the next one.

However the dynamics of $\mathbf{V}$ may be sometimes approximated from heuristics and described by an evolution equation:

$$\frac{\partial \mathbf{V}}{\partial t} + \mathbb{M}(\mathbf{V}) = 0 \tag{7}$$

The operator $\mathbb{M}$ is named *evolution model*. Given an initial condition for $\mathbf{V}$ at time $t = 0$, it is possible to compute $\mathbf{V}$ at any time $t > 0$ by integrating (7). The Tikhonov regularization, corresponding to the second term of (6), is no more required.

Depending on the experimental context, various evolution models may be considered. The best would be to consider the mathematical equations describing the observed physical processes. For instance in oceanography, the heat equation rules the diffusion of the surface temperature and the shallow-water equations describe the ocean surface circulation Huot et al. (2008). These shallow-water equations are a simplification of the Navier-Stokes equation describing turbulent and incompressible fluid flows:

$$\rho \frac{d\mathbf{V}}{dt} = \mathbf{F} - \nabla p + \mu \nabla^2 \mathbf{V} \tag{8}$$

F being the gravity force, p the pressure, ρ the fluid density, and μ the kinetic viscosity. Without effective knowledge on dynamics, simpler equations can be experimented, as the Lagrangian constancy:

$$\frac{d\mathbf{V}}{dt} = \frac{\partial \mathbf{V}}{\partial t} + (\mathbf{V}^T \nabla)\mathbf{V} = 0, \tag{9}$$

However these evolution models are often an approximation of the reality and deviations to them must be allowed during the computation, as it is the case with weak data assimilation techniques. Equation (9) is considered in the remainder of the paper.

3 Data Assimilation

Let $\mathbf{X}$ be the state vector and $\mathbf{Y}$ the observation vector defined on a spatio-temporal domain $A = \Omega \times [0, T]$. Data Assimilation solves the following system of three equations:

$$\begin{aligned} \frac{\partial \mathbf{X}}{\partial t}(\mathbf{x}, t) + \mathbb{M}(\mathbf{X})(\mathbf{x}, t) &= \mathcal{E}_m(\mathbf{x}, t) && (11)\\ \mathbb{H}(\mathbf{Y}, \mathbf{X})(\mathbf{x}, t) &= \mathcal{E}_o(\mathbf{x}, t) && (12)\\ \mathbf{X}(\mathbf{x}, 0) &= \mathbf{X}_b(\mathbf{x}) + \mathcal{E}_b(\mathbf{x}) && (13) \end{aligned}$$

In addition to the evolution and observation equations (Eqs. (11,12)), a constraint on the initial condition, Eq. (13), is added. For linking with the previous section, Eq. (11) and Eq. (12) respectively correspond to Eq. (7) and Eq. (3) with $\mathbf{X} = \mathbf{V}$ and $\mathbf{Y} = I$ in the case of motion estimation from image data. An error term is added to each equation: $\mathcal{E}_m$ represents the deviation to the evolution equation, $\mathcal{E}_o$ describes the errors on observation data and the deviation from the observation equation, and $\mathcal{E}_b$ concerns the initial condition uncertainty. These errors are supposed unbiased and Gaussian, and fully characterized by their covariance matrix Q, R and B. For solving the full system, the functional (10) has to be minimized with respect to $\mathbf{X}$. Its differential is established by determining the directional derivative and introducing the auxiliary variable (named *adjoint variable*) $\lambda(\mathbf{x}, t) = \displaystyle\int_A Q^{-1}(\mathbf{x}, t, \mathbf{x}', t') \left(\frac{\partial \mathbf{X}}{\partial t} + \mathbb{M}(\mathbf{X}) \right) (\mathbf{x}', t') d\mathbf{x}' dt'$. As operators $\mathbb{M}$ and $\mathbb{H}$ are non linear, a local linearization is applied: the state vector is written as $\mathbf{X} = \mathbf{X}_b + \delta\mathbf{X}$, with $\mathbf{X}_b$ the *background variable* and $\delta\mathbf{X}$ the *incremental variable*. A Taylor development of $\mathbb{M}$ and $\mathbb{H}$ is performed at

$$\begin{aligned} E(\mathbf{X}) = &\int_A \int_A \big(\frac{\partial \mathbf{X}}{\partial t} + \mathbb{M}(\mathbf{X})\big)^T (\mathbf{x}, t) Q^{-1}(\mathbf{x}, t, \mathbf{x}', t') \big(\frac{\partial \mathbf{X}}{\partial t} + \mathbb{M}(\mathbf{X})\big)(\mathbf{x}', t') d\mathbf{x} dt d\mathbf{x}' dt' \\ &+ \int_A \int_A \mathbb{H}(\mathbf{X}, \mathbf{Y})^T (\mathbf{x}, t) R^{-1}(\mathbf{x}, t, \mathbf{x}', t') \mathbb{H}(\mathbf{X}, \mathbf{Y})(\mathbf{x}', t') d\mathbf{x} dt d\mathbf{x}' dt' \\ &+ \int_\Omega \int_\Omega \big(\mathbf{X}(\mathbf{x}, 0) - \mathbf{X}_b(\mathbf{x})\big)^T B^{-1}(\mathbf{x}, \mathbf{x}') \big(\mathbf{X}(\mathbf{x}', 0) - \mathbf{X}_b(\mathbf{x}')\big) d\mathbf{x} d\mathbf{x}' \end{aligned} \tag{10}$$

the neighborhood of $\mathbf{X}_b$. The following system of equations has then to be solved (reader is referred to Béréziat and Herlin (2010); Valur Hólm (2003) for a complete description):

$$\lambda(\mathbf{x}, \mathbf{T}) = 0 \tag{14}$$

$$-\frac{\partial \lambda}{\partial t} + \left(\frac{\partial \mathbb{M}}{\partial \mathbf{X}}\Big|_{\mathbf{X}_b}\right)^* \lambda = -\int_A \left(\frac{\partial \mathbb{H}}{\partial \mathbf{X}}\Big|_{\mathbf{X}_b}\right)^* R^{-1} \left(\mathbb{H}(\mathbf{X}_b, \mathbf{Y}) + \frac{\partial \mathbb{H}}{\partial \mathbf{X}}\Big|_{\mathbf{X}_b}(\delta \mathbf{X})\right) d\mathbf{x}' dt' \tag{15}$$

$$\mathbf{X}_b(\mathbf{x}, 0) = \mathbf{X}_b(\mathbf{x}) \tag{16}$$

$$\frac{\partial \mathbf{X}_b}{\partial t} + \mathbb{M}(\mathbf{X}_b) = 0 \tag{17}$$

$$\delta \mathbf{X}(\mathbf{x}, 0) = \int_\Omega B\lambda(\mathbf{x}', 0) d\mathbf{x}' \tag{18}$$

$$\frac{\partial \delta \mathbf{X}}{\partial t} + \frac{\partial \mathbb{M}}{\partial \mathbf{X}}\Big|_{\mathbf{X}_b}(\delta \mathbf{X}) = \int_A Q\lambda(\mathbf{x}', t') d\mathbf{x}' dt' \tag{19}$$

Operators $\left(\frac{\partial \mathbb{M}}{\partial \mathbf{X}}\right)^*$ and $\left(\frac{\partial \mathbb{H}}{\partial \mathbf{X}}\right)^*$ are the *adjoint operators*. For a given operator $\mathbb{K}$, the adjoint is mathematically defined by:

$$\langle \mathbb{K}(\eta)), \lambda \rangle = \langle \eta, \mathbb{K}^*(\lambda) \rangle \tag{20}$$

The linearization of operators $\mathbb{M}$ and $\mathbb{H}$ leads to an inexact solution of Equations (14) to (19) and requires to iterate this incremental method. The background variable is first computed from Equations (16) and (17). Background and incremental variables are used to compute the adjoint variable with Equations (14) and (15). After updating the background variable with $\mathbf{X}_b = \mathbf{X}_b + \delta \mathbf{X}$, a new value for the incremental variable can then be computed from Equations (18) and (19). The process is iterated up to convergence. This method, named incremental 4D-var, has been designed specifically to solve non linear evolution and observation models such as those discussed in the previous section.

4 The error covariance matrix

This section describes the use of error covariance matrices to handle noisy data and to express spatio-temporal regularity properties.

First, for a general discussion, let Z be a stochastic state vector depending on the spatial coordinate $\mathbf{x}$ and Σ its covariance matrix:

$$\Sigma(\mathbf{x}, \mathbf{x}') = \iint \left(Z(\mathbf{x}) - \mathbb{E}(Z)\right)^T \left(Z(\mathbf{x}') - \mathbb{E}(Z)\right) dP(\mathbf{x}, \mathbf{x}')$$

$dP(\mathbf{x}, \mathbf{x}')$ being the density of $(Z(\mathbf{x}), Z(\mathbf{x}'))$ and $\mathbb{E}$ the expectation. The inverse of Σ is defined in Oliver (1998) by:

$$\int \Sigma^{-1}(\mathbf{x}, \mathbf{x}'')\Sigma(\mathbf{x}'', \mathbf{x}') d\mathbf{x}'' = \delta(\mathbf{x} - \mathbf{x}') \tag{21}$$

A first class of covariance matrices concerns the one depending on $\mathbf{x}-\mathbf{x}'$: $\Sigma(\mathbf{x},\mathbf{x})' = \Sigma(\mathbf{x}-\mathbf{x}')$. Equation (21) can be rewritten as a convolution product $\int \Sigma^{-1}(r-r')\Sigma(r')dr' = \delta(r)$ with $r = \mathbf{x}-\mathbf{x}'$ and $r' = \mathbf{x}''-\mathbf{x}'$. This corresponds to a simple product $\widehat{\Sigma}^{-1}(\omega)\widehat{\Sigma}(\omega) = 1$ in the Fourier space. It is then much easier to compute the inverse covariance matrix in the Fourier domain. A Dirac covariance, $\Sigma(\mathbf{x},\mathbf{x}') = \delta(\mathbf{x}-\mathbf{x}')$, has an inverse which is also a Dirac function, and we have $\iint Z^T(\mathbf{x})\Sigma^{-1}Z(\mathbf{x}')d\mathbf{x}d\mathbf{x}' = \int \|Z(\mathbf{x})\|^2 d\mathbf{x}$. Applying a Dirac covariance is therefore equivalent to a zero-order regularization. For an exponential covariance, $\Sigma(\mathbf{x},\mathbf{x}') = \exp\left(-\frac{\|\mathbf{x}-\mathbf{x}'\|}{\sigma}\right)$, we have $\iint Z^T(\mathbf{x})\Sigma^{-1}Z(\mathbf{x}')d\mathbf{x}d\mathbf{x}' = \int \frac{1}{2\sigma}\left(\|Z(\mathbf{x})\|^2 + \sigma^2\|\nabla Z(\mathbf{x})\|^2\right)d\mathbf{x}$ Bérériat and Herlin (2010), which is equivalent to a first-order regularization.
A second class concerns covariance matrices written as $\Sigma(\mathbf{x},\mathbf{x}') = S(\mathbf{x})\delta(\mathbf{x}-\mathbf{x}')$. We have $\Sigma^{-1}(\mathbf{x},\mathbf{x}') = \delta(\mathbf{x}-\mathbf{x}')S^{-1}(\mathbf{x})$. In this case, the error is localized. These matrices are used to weight the contribution of pixels in the energy function (10).

To avoid noisy data having an impact on the solution, we define the inverse of the observation covariance matrix R as:

$$R^{-1}(\mathbf{x},t;\mathbf{x}',t') = \delta(\mathbf{x}-\mathbf{x}')\delta(t-t')f(\mathbf{x},t) \tag{22}$$

with f a confidence measure which is close to 0 if the observation value must be discarded because the acquisition process failed or the observation model is wrong. A first category of pixels is identified from metadata with a function f_{sensor} that expresses the quality of the acquisition. For example SST images contain clouds occluding the ocean surface: these areas are flagged by the provider and f_{sensor} has a low value on these pixels. A second category concerns pixels having a small value of the space-time gradient norm: Equation (2) becomes true whatever the value of $\mathbf{V}$ as it reduces to $0 = 0$. To discard these pixels from the computation we define the quality function $f_{\mathbb{H}}$ such as:

$$f_{\mathbb{H}}(\mathbf{x},t) = 1 - \exp\left(-\frac{\|\nabla_3 I(\mathbf{x},t)\|^2}{\sigma}\right) \tag{23}$$

with ∇_3 the gradient operator on the space-time domain. The function f in Eq. (22) is then defined by $f(\mathbf{x},t) = f_{\text{sensor}}(\mathbf{x},t)f_{\mathbb{H}}(\mathbf{x},t)$.

Another concern is the spatial regularization of the result. Our objective is to perform this regularization with the observation error covariance matrix R. Applying a spatial regularization to the state vector $\mathbf{X}$ may be seen as defining a piecewise constant approximation $\mathbf{X}_{\text{pc}}$. This issue is formalized by extending the observation vector as $\mathbf{Y}' = (\mathbf{Y},0)^T$: the observations $\mathbf{Y}$ will be compared to $\mathbf{X}$ as previously and null observations of $\nabla\mathbf{X}$ are given in order to force $\mathbf{X}$ to be piecewise constant. For the optical flow estimation, the observation equation is rewritten as:

$$\mathbb{H}'(\mathbf{V},I) = \begin{pmatrix} I(\mathbf{x}+\mathbf{V},t+1) - I(\mathbf{x},t) \\ \nabla\mathbf{V} \end{pmatrix} = \mathcal{E}_o \tag{24}$$

This is a two-component equation and the inverse of the error covariance matrix is defined as:

$$R'(\mathbf{x},t;\mathbf{x}',t') = \begin{pmatrix} R^{-1}(\mathbf{x},t;\mathbf{x}',t') & 0 \\ 0 & \gamma\delta(\mathbf{x}-\mathbf{x}') \end{pmatrix} \tag{25}$$

with $\gamma > 0$ and R^{-1} written as in Eq. (22). Using $\mathbb{H}'$ and R'^{-1} from Eq. (24) and (25), with $\gamma = \alpha^2$, we have:

$$\begin{aligned} \iint \mathbb{H}'(\mathbf{X},\mathbf{Y}')^T R'^{-1} \mathbb{H}'(\mathbf{X},\mathbf{Y}') d\mathbf{x}dtd\mathbf{x}'dt' = \\ \int \left(f(\mathbf{x},t)(I(\mathbf{x}+\mathbf{V},t+1) - I(\mathbf{x},t))^2 + \alpha^2 \|\nabla\mathbf{V}\|^2 \right) d\mathbf{x}dt \end{aligned} \tag{26}$$

The second part of this integral may be recognized as the classical Tikhonov regularization involved in Eq. (4). The data assimilation method, applied on the state vector $\mathbf{X}$, with the observation $\mathbf{Y}'$ and the matrix R', actually performs the same regularization in an indirect way.

5 Implementation and Results

Details for determining the differential and adjoint operator of $\mathbb{M}(\mathbf{V}) = \nabla\mathbf{V}^T\mathbf{V}$ are given in Béréziat and Herlin (2010). The differential of $\mathbb{H}(\mathbf{V},I) = I(\mathbf{x}+\mathbf{V},t+1) - I(\mathbf{x},t)$ is $\nabla I^T(\mathbf{x}+\mathbf{V},t+1) \stackrel{\text{def}}{=} \nabla I^T \circ \mathbf{V}$ Brox et al. (2004) and the adjoint operator is the transpose. A Dirac covariance is chosen for Q and B. Equations (17,15,19) correspond to the three following EDPs:

$$\frac{\partial\mathbf{V}}{\partial t} + \mathbf{V}_b^T\nabla\mathbf{V}_b = 0 \tag{27}$$

$$-\frac{\partial\lambda}{\partial t} - \nabla\lambda^T\mathbf{V}_b - \lambda^T\nabla^\perp\mathbf{V}_b = L \tag{28}$$

$$\frac{\partial\delta\mathbf{V}}{\partial t} + \mathbf{V}_b^T\nabla\delta\mathbf{V} + \nabla\mathbf{V}_b^T\delta\mathbf{V} = \lambda \tag{29}$$

The right member of Equation (28) is:

$$L = -\nabla I \circ \mathbf{V}_b \left(I\circ\mathbf{V}_b - I + \nabla I^T \circ \mathbf{V}_b\delta\mathbf{V} \right) f_{\mathbb{H}} f_{\text{sensor}}$$

Discretisation is performed as follows. Equation (27) is a non linear advection and a robust explicit numerical scheme is proposed in Béréziat and Herlin (2010). Equations (28) and (29) have linear but non constant advection terms with additional forcing terms. The advection terms are discretized using an upwind scheme Ames (1977).

The initial condition $\mathbf{X}_b$, in Equation (16), is given by the Horn & Schunck algorithm Horn and Schunk (1981).

5.1 Synthetic data

The potential of the method is first demonstrated on a synthetic sequence displaying two squares, one moving down and the other moving up, meeting each other on the last frames. Figures 1(a) and 1(b) show the results obtained at

the beginning and the end of the sequence for Horn & Schunck (HS) and Data Assimilation (DA) methods. HS has the drawback of spatially smoothing the velocity field at the junction of the two squares at the end of the sequence producing sometimes a wrong direction for the motion vector. The heuristics on the dynamics is successfully exploited by DA that estimates a correct direction of the motion field.

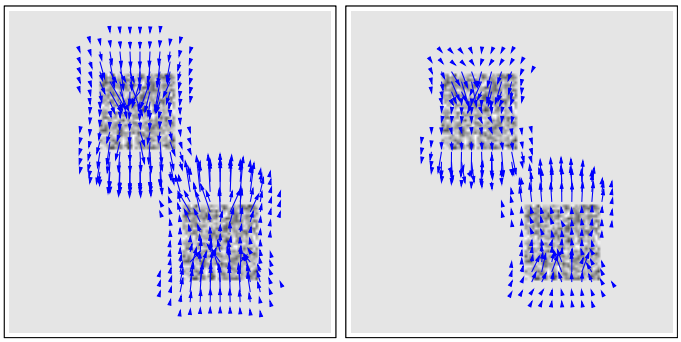

(a) Result on frame 3 for HS(left) DA (right).

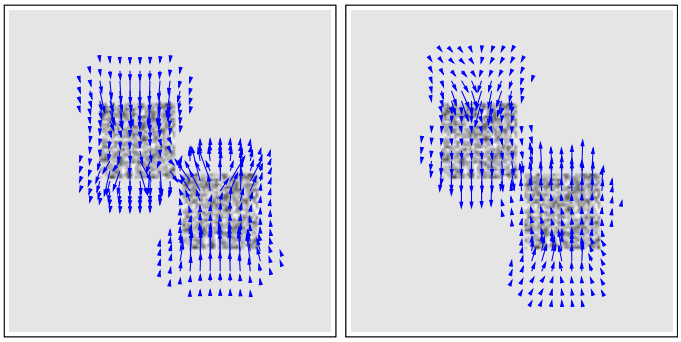

(b) Result on frame 9 for HS (left) and DA (right).

Figure 1: Results on synthetic data.

5.2 Satellite data

The algorithm has also been used on a sequence of 17 SST images, acquired by NOAA-AVHRR in July 1998 over the Black Sea. The image data present major difficulties: (1) Figure 2(a) and 2(b) display two consecutive frames with a cloud occluding a large region and displaying a large displacement; (2) Figure 2(c) shows data missing due to a registration problem; (3) the pixel brightness is subject to large variations on the sequence due to varying acquisition times and atmospheric conditions (see frame 10 in Figure 2(d) which is darker than other frames). To deal with this last problem, we use the coarse hypothesis of constant brightness variation along the trajectory: $\frac{dI}{dt} = a$, with a being a real constant. Consequently $\frac{\partial}{\partial x}\left(\frac{dI}{dt}\right) = \frac{d}{dt}\left(\frac{\partial I}{\partial t}\right) = 0$ and we consider $\frac{\partial I}{\partial x}$ as input data instead of the image function I.

For analyzing results, we focus on a small region of interest, marked by the blue square in Figure 2(b). Magnification is displayed at several acquisition

dates in Figure 2(d). It shows a black structure evolving with a translational motion, from right to left, during the first frames and then with a counter clockwise rotational motion during the remainder of the sequence. The acquisitions also display missing data on frames 9 and 11. Figure 3 shows the results of HS and DA on the second frame. The two methods give similar results. This demonstrates that the spatial regularity involved in HS may be suppressed and replaced by the evolution equation if the dynamics is correctly modeled. Figure 4 displays the results obtained on the third and fourth frames (partially occluded by a cloud). As HS computes spatio-temporal gradients using consecutive frames, it fails if gradients are computed on missing data. DA, however, provides a good result because these pixels are discarded due to the confidence function f: the solution is obtained from the evolution equation. Figure 5 illustrates results on the tenth and eleventh frames with many missing pixels. HS fails to provide a coherent velocity field. DA successes again thanks to the evolution equation and the discard of missing data.

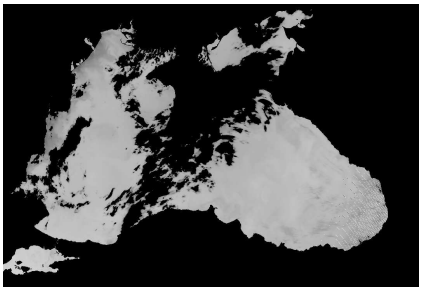

(a) Large cloud in black occluding the Sea.

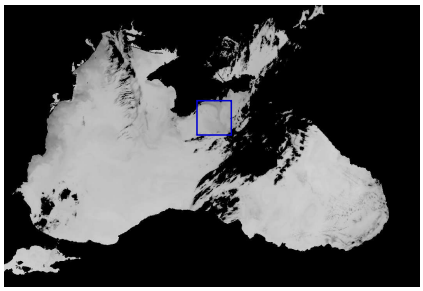

(b) Next frame.

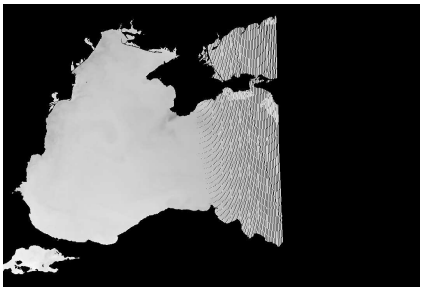

(c) Missing data on the right part of the acquisition.

(d) Region of interest on frames 2, 3, 4, 9, 10 and 11.

Figure 2: SST sequence with noisy data.

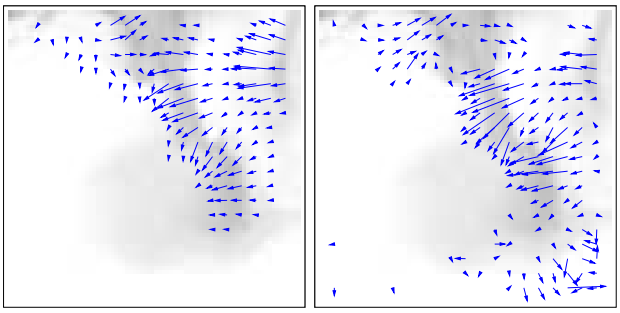

Figure 3: Result on SST with HS (left) and DA (right) on frame 2.

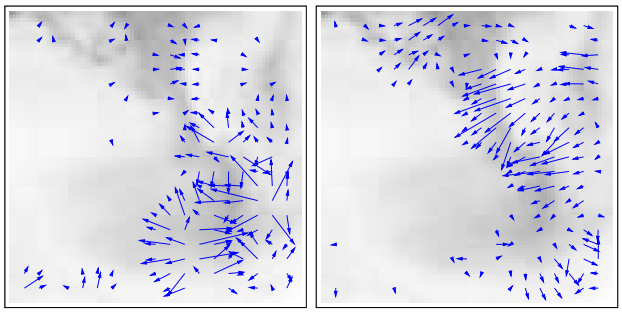

(a) Frame 3.

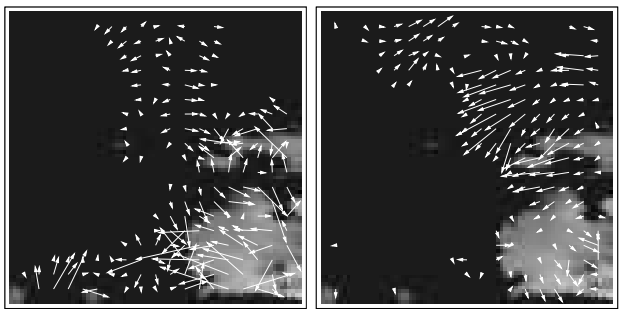

(b) Frame 4.

Figure 4: Cloud occultation: HS (left) and DA (right).

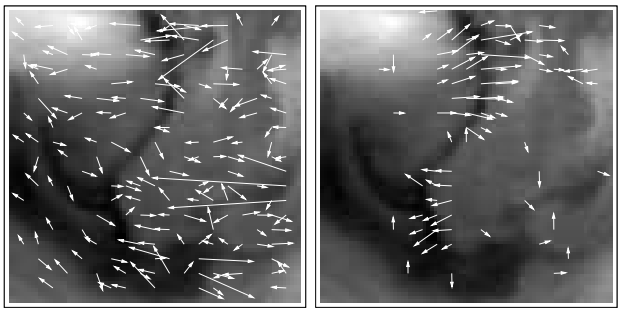

(a) Frame 10.

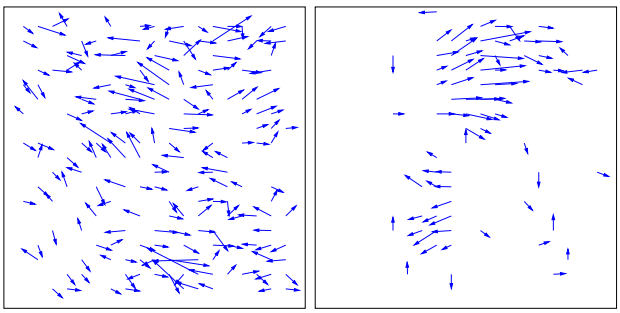

(b) Frame 11. The background – see frame 11 in Figure 2(d) – has been removed in order to enhance visibility.

Figure 5: Missing data: HS (left) and DA (right).

6 Concluding remarks

In the paper, we proposed a method to estimate large displacements from an image sequence including some noisy data. The method relies on an evolution equation which approximately describes the image dynamics. Data assimilation is used to simultaneously solve the evolution and brightness transport equations. Noisy data are identified by a confidence function and discarded from the computation of the solution, that is then estimated from the evolution equation on these pixels. A spatial regularization of the solution may be obtained from a suitable observation equation and its covariance matrix. We discussed the relevance of the method on satellite images displaying various types of missing data. As the dynamics is obtained from heuristics, we allowed inaccuracies of the evolution equation by involving a model error in the equations. Even if the dynamics' model is inaccurate, we obtain better results than standard optical flow methods because the missing data are correctly managed by our method.

The major perspective is to define an evolution model dealing with spatio-temporal discontinuities of the dynamics. If the state vector is too different from the observations at a given time step, the method should consider a dynamics' discontinuity and the evolution equation should no more be involved in the computation of the solution. This could be obtained by increasing the error model and its covariance matrix Q. However the problem will then become ill-posed and require a spatial regularization at that time step. The difficulty is to define adaptive covariances Q and R driven by the observations and the state vector in order to release the weight of the evolution equation and to apply regularization if necessary.

References

Ames, W. (1977). *Numerical Methods for Partial Differential Equations*. Academic Press.

Bérériat, D. and Herlin, I. (2010). Solving ill-posed image processing problems using data assimilation. *Numerical Algorithms*, to appear.

Bérériat, D., Herlin, I., and Younes, L. (2000). A generalized optical flow constraint and its physical interpretation. In *CVPR*, pages 487–492.

Brox, T., Bruhn, A., Papenberg, N., and Weickert, J. (2004). High accuracy optical flow estimation based on a theory for warping. In *ECCV*, volume 4, pages 25–36.

Horn, B. and Schunk, B. (1981). Determining optical flow. *Artificial Intelligence*, 17:185–203.

Huot, E., Herlin, I., and Korotaev, G. (2008). Assimilation of SST satellite images for estimation of ocean circulation velocity. In *IGARSS*.

Isambert, T., Berroir, J., and Herlin, I. (2008). A multiscale vector spline method for estimating the fluids motion on satellite images. In *ECCV*. Springer.

Odobez, J.-M. and Bouthemy, P. (1998). Direct incremental model-based image motion segmentation for video analysis. *Signal Processing*, 66(2):143–155.

Oliver, D. (1998). Calculation of the inverse of the covariance. *Mathematical Geology*, 30(7):911–933.

Papadakis, N., Corpetti, T., and Mémin, E. (2007a). Dynamically consistent optical flow estimation. In *ICCV*.

Papadakis, N., Héas, P., and Mémin, E. (2007b). Image assimilation for motion estimation of atmospheric layers with shallow-water model. In *ACCV*, pages 864–874.

Proesmans, M., Van Gool, L., Pauwels, E., and Oosterlinck, A. (1994). Determination of optical flow and its discontinuities using non-linear diffusion. In *ECCV*, volume 2, pages 295–304.

Tikhonov, A. N. (1963). Regularization of incorrectly posed problems. *Sov. Math. Dokl.*, 4:1624–1627.

Valur Hólm, E. (2003). Lectures notes on assimilation algorithms. Technical report, European Centre for Medium-Range Weather Forecasts Reading.

Wildes, R. and Amabile, M. (1997). Physically based fluid flow recovery from image sequences. In *CVPR*, pages 969–975.

Centre de recherche INRIA Paris – Rocquencourt
Domaine de Voluceau - Rocquencourt - BP 105 - 78153 Le Chesnay Cedex (France)

Centre de recherche INRIA Bordeaux – Sud Ouest : Domaine Universitaire - 351, cours de la Libération - 33405 Talence Cedex
Centre de recherche INRIA Grenoble – Rhône-Alpes : 655, avenue de l'Europe - 38334 Montbonnot Saint-Ismier
Centre de recherche INRIA Lille – Nord Europe : Parc Scientifique de la Haute Borne - 40, avenue Halley - 59650 Villeneuve d'Ascq
Centre de recherche INRIA Nancy – Grand Est : LORIA, Technopôle de Nancy-Brabois - Campus scientifique
615, rue du Jardin Botanique - BP 101 - 54602 Villers-lès-Nancy Cedex
Centre de recherche INRIA Rennes – Bretagne Atlantique : IRISA, Campus universitaire de Beaulieu - 35042 Rennes Cedex
Centre de recherche INRIA Saclay – Île-de-France : Parc Orsay Université - ZAC des Vignes : 4, rue Jacques Monod - 91893 Orsay Cedex
Centre de recherche INRIA Sophia Antipolis – Méditerranée : 2004, route des Lucioles - BP 93 - 06902 Sophia Antipolis Cedex

Éditeur
INRIA - Domaine de Voluceau - Rocquencourt, BP 105 - 78153 Le Chesnay Cedex (France)
http://www.inria.fr
ISSN 0249-6399